

# Topological Defect Inflation\*

Nobuyuki Sakai†

*Yukawa Institute for Theoretical Physics, Kyoto University, Kyoto 606-8502*

## Abstract

We address some issues of topological defect inflation. (1) We clarify the causal structure of an inflating magnetic monopole. The spacetime diagram shows explicitly that this model is free from the “graceful exit” problem, while the monopole itself undergoes “eternal inflation”. (2) We extend the study of inflating topological defects to Brans-Dicke gravity. Contrary to the case of Einstein gravity, any inflating monopole eventually shrinks and takes a stable configuration. (3) We reanalyze chaotic inflation with a non-minimally coupled massive scalar field. We find a new solution of domain wall inflation, which relaxes constraints on the coupling constant for successful inflation.

## 1 Introduction

Guendelman & Rabinowitz, Linde, and Vilenkin independently claimed that topological defects expand exponentially if the vacuum expectation value of the Higgs field  $\eta$  is of the order of the Planck mass  $m_{\text{Pl}}$  [1, 2]. Their arguments were later verified in numerical simulations [3, 4]: it was shown in particular that the critical value of  $\eta$  for domain walls and global monopoles is  $\eta_{\text{inf}} \approx 0.33m_{\text{Pl}}$ , regardless of initial conditions.

Because this “topological defect inflation” (TDI) model is free from the fine-tuning problem of initial conditions, it has been attracting attention. In particular, recently it has been argued that TDI takes place in some of the plausible models in particle physics [5].

In this paper, concerning the TDI model, we address the following three issues.

- (1) Causal structure of an inflating magnetic monopole [6].
- (2) TDI in Brans-Dicke (BD) theory [7].
- (3) TDI induced by non-minimally coupled massive scalar field [8].

## 2 Causal Structure of an Inflating Magnetic Monopole

Among various topological defects, spacetime solutions of magnetic monopoles have been studied the most intensively in the literature [9, 10, 11]. This originated from the rather mathematical interest in static solutions with non-Abelian hair [9]. It was shown [10] that static regular solutions are nonexistent if  $\eta$  is larger than a critical value  $\eta_{\text{sta}} (\sim m_{\text{Pl}})$ . Our previous work [4] revealed the properties of monopoles for  $\eta > \eta_{\text{sta}}$ . There are three types of solutions, depending on coupling constants and initial configuration: a monopole either expands, collapses into a black hole, or comes to take a stable configuration. The first type corresponds to TDI.

Recently, the causal structure of an inflating magnetic monopole was discussed in Ref.[12]. The spacetime diagrams in Ref.[12] showed, for instance, that the inflationary boundary expands along outgoing null geodesics, that is, no observer can exit from an inflationary region. The above argument would be fatal to TDI because it implies that reheating never occurs. Therefore, the spacetime structure of TDI deserves close examination. Here we discuss the causal structure of an inflating magnetic monopole, based on the numerical solution in Ref.[4].

In order to see the spacetime structure for numerical solutions, we observe the signs of the expansion of a null geodesic congruence. For a spherically symmetric metric,

$$ds^2 = -dt^2 + A^2(t, r)dr^2 + B^2(t, r)r^2(d\theta^2 + \sin^2\theta d\varphi^2), \quad (1)$$

---

\*This talk is based on Refs.[6, 7, 8].

†E-mail:sakai@yukawa.kyoto-u.ac.jp

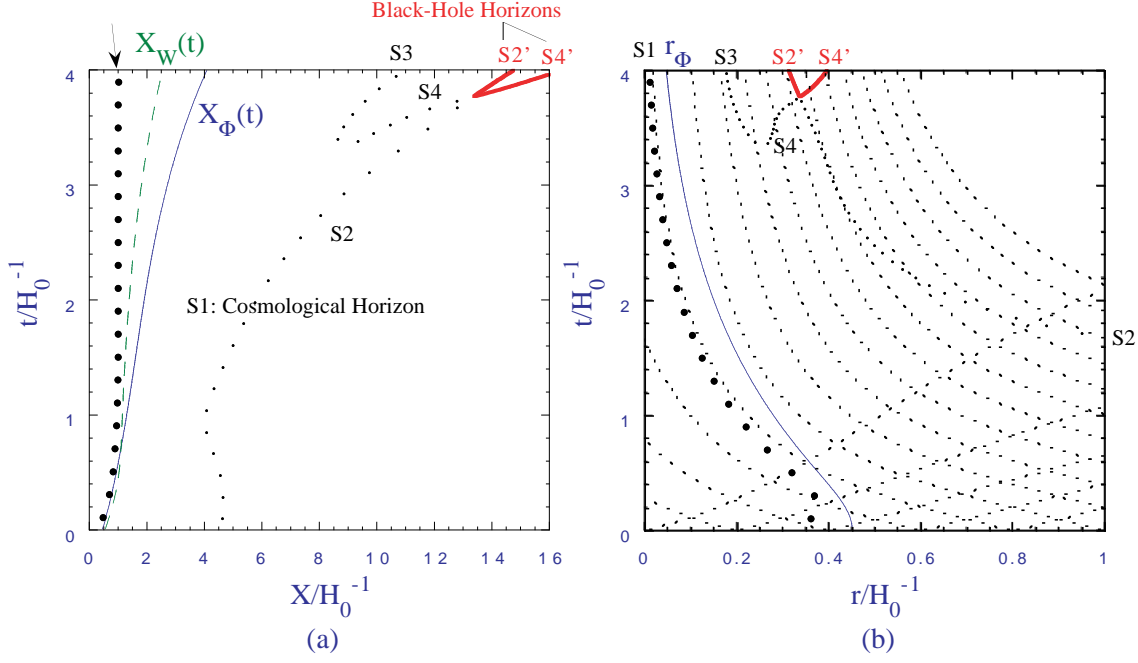


Figure 1: A solution of an inflating magnetic monopole. (a) is the reproduction of Fig. 4(a) of [4]: we plot the trajectories of monopole boundaries and of apparent horizons in terms of the proper distance from the center,  $X$ ; dotted lines denote apparent horizons; we normalize time and length by the horizon scale defined as  $H_c^{-1} \equiv [8\pi V(0)/3m_{\text{Pl}}^2]^{-1/2}$ . In (b) we plot ingoing and outgoing null geodesics (dotted lines) besides the above-mentioned trajectories in a  $t - r$  diagram; the boundary moves *inward* and eventually becomes *spacelike*.

an outgoing (+) or ingoing (-) null vector is given by  $k_\pm^\mu = (1, \pm A^{-1}, 0, 0)$ , and its expansion  $\Theta_\pm$  is written as

$$\Theta_\pm = k_{\pm;\theta}^\theta + k_{\pm;\varphi}^\varphi = \frac{2}{B} \left( \frac{\partial B}{\partial t} \pm \frac{1}{Ar} \frac{\partial(Br)}{\partial r} \right), \quad (2)$$

which is defined as the trace of a *projection* of  $k_{;\nu}^\mu$  onto a relevant 2-dimensional surface [13]. We define an ‘‘apparent horizon’’ as the surface with  $\Theta^+ = 0$  or  $\Theta^- = 0$ <sup>‡</sup>. We label those surfaces as S1, S2, etc. in our figures.

In Fig. 1(a), we plot the trajectories of monopole boundaries and of apparent horizons in terms of the proper distance from the center:  $X \equiv \int_0^r A dr'$ . Here we define the boundary in two ways:  $X_\phi$  as the position of  $\phi = \eta/2$  and  $X_w$  as the position of  $w = 1/2$ , where  $\phi$  and  $w$  are the Higgs field and a gauge-field function, respectively. An apparent horizon S1 almost agrees with  $X = H_c^{-1} \equiv [8\pi V(0)/3m_{\text{Pl}}^2]^{-1/2}$ , which implies that the monopole core is almost de Sitter spacetime. Figure 1(a) also illustrates that a wormhole structure with black hole horizons appears around an inflating core. Because the inflating core becomes causally disconnected from the outer universe, such an isolated region is called a ‘‘child universe’’. The production of child universes was originally discussed by Sato, Sasaki, Kodama, and Maeda [14] in the context of old inflation [15].

To see the causal structure of the inflating monopole more closely, we also plot ingoing and outgoing null geodesics in Fig. 1(b). An important feature for the magnetic monopole as well as the global monopole [16] is that the boundary moves *inward* and, moreover, it eventually becomes *spacelike*.

To understand the global structure, which is not completely covered by the numerical solution, we make a reasonable assumption that the core region approaches to de Sitter spacetime and the outside to Reissner-Nordström, as in Refs.[11, 12]. In each static spacetime, apparent horizons and event horizons are identical; the signs of  $(\Theta^+, \Theta^-)$  are determined as is shown in Fig. 2. The above assumption implies

<sup>‡</sup> In the literature an ‘‘apparent horizon’’ usually refers to the outermost surface with  $\Theta^+ = 0$  in an asymptotically flat spacetime. In this article, however, we call any marginal surface with  $\Theta^+ = 0$  or  $\Theta^- = 0$  an apparent horizon.

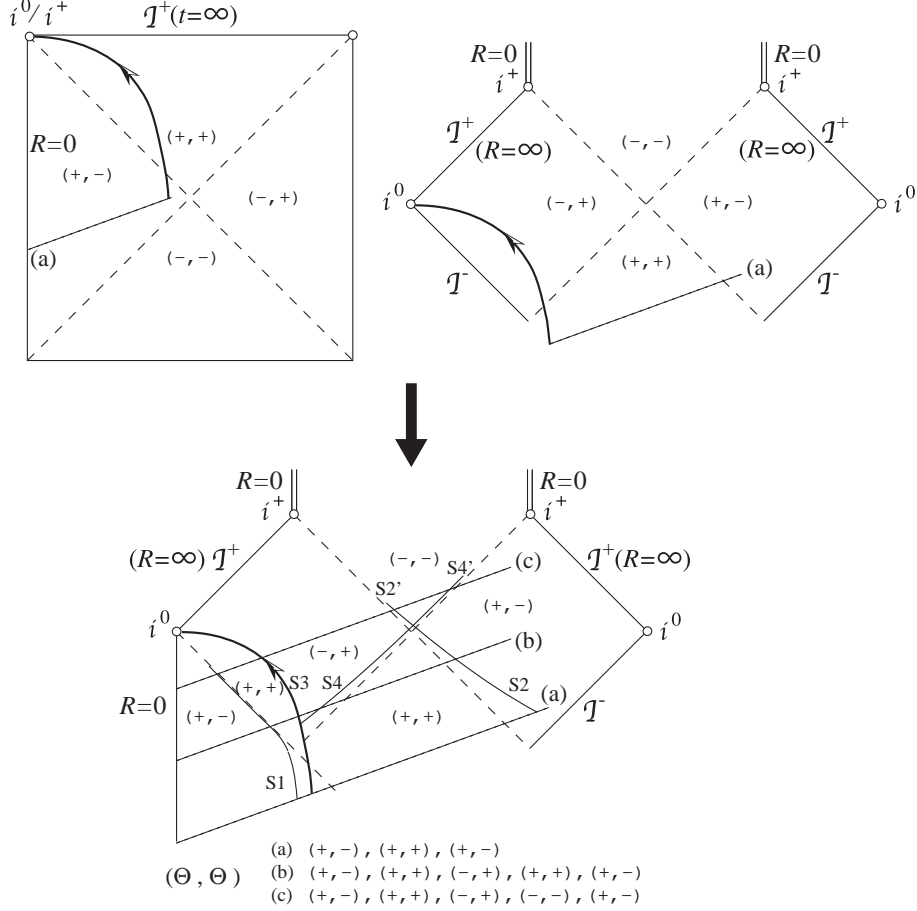


Figure 2: Possible conformal diagram for the spacetime of an inflating magnetic monopole. The core region is approximated to be de Sitter spacetime and the outside to be Reissner-Nordström. The upper figure shows how the monopole boundary is embedded in each spacetime separately, and the lower figure shows a complete spacetime.  $\mathcal{I}^+$  and  $\mathcal{I}^-$  represent future and past null infinity,  $i^+$  represents future timelike infinity, and  $i^0$  represents spacelike infinity. Long-dashed lines denote event horizons, which are identified with apparent horizons in de Sitter or Reissner-Nordström spacetime. Short-dashed lines (a), (b), and (c) denote time-slices, which correspond to the embedding diagrams (a), (b), and (c) of Fig. 5 of [4], respectively. For reference, we schematically depict the trajectories of apparent horizons. We also write down the signs of the expansion  $\Theta$ . The structure of apparent horizons, which is determined by the signs of  $\Theta^\pm$ , completely agrees with that in Fig. 1 and Fig. 5 of [4].

that, although the whole space in the early stage is quite dynamical and an apparent horizon does not coincide with an event horizon, the two horizons later approach each other. Hence, we can extrapolate the global structure from the structure of apparent horizons in the local numerical solution. From the consistency of the spatial distribution of the signs of  $(\Theta^+, \Theta^-)$ , we conclude that Fig. 2 gives the only possible embedding.

Cosmologically, Fig. 2 tells us that any inflationary region eventually enters a reheating phase because any observer inside the core finally goes out. On the other hand, the monopole boundary continues to expand in terms of the physical size and approaches spatial infinity ( $i^0$ ). Figure 2 thus proves that this model is free from the “graceful exit” problem, while the monopole itself undergoes “eternal inflation”.

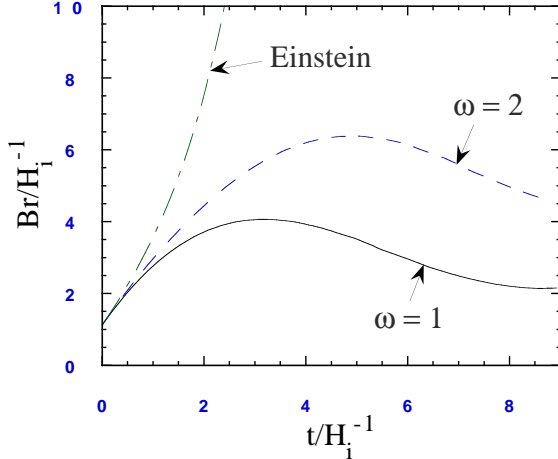


Figure 3: Dynamics of a global monopole for several values of  $\omega$ . We set  $\lambda = 0.1$  and  $\eta/m_{\text{Pl}}(\Phi_i) = 1$ . We plot trajectories of the position of  $\phi = \eta/2$ .

### 3 Topological Defect Inflation in Brans-Dicke Theory

The Brans-Dicke-Higgs system, which we consider here, is described by the action

$$S = \int d^4x \sqrt{-g} \left[ \frac{\Phi}{16\pi} \mathcal{R} - \frac{\omega}{16\pi\Phi} (\nabla_\mu \Phi)^2 - \frac{1}{2} (\nabla_\mu \phi^a)^2 - V(\phi) \right], \quad \text{with } V(\phi) = \frac{\lambda}{4} (\phi^a \phi^a - \eta^2)^2, \quad (3)$$

where  $\Phi$  and  $\omega$  are the BD field and the BD parameter, respectively.

In extended inflation [17], where the BD theory was originally introduced in inflationary cosmology, the universe does not expand exponentially but expands with a power law. This slower expansion solved the graceful exit problem of old inflation [15]. We thus expect that the BD field also affects the dynamics and global spacetime structure of inflating monopoles.

Let us begin with a discussion of the fate of an inflating topological defect. Once inflation begins, the core region can be approximated to be a homogeneous spacetime, where the scale factor and the BD field are described by the solution of extended inflation [17]:  $a(t) \propto t^{\omega+\frac{1}{2}}$ ,  $\Phi(t) \propto t^2$ . Hence, the effective Planck mass,

$$m_{\text{Pl}}(\Phi) = \sqrt{\Phi} \propto a^{\frac{1}{\omega+\frac{1}{2}}}, \quad (4)$$

continues to increase until inflation ends. This implies that, even if  $\eta/m_{\text{Pl}}(\Phi)$  is large enough to start inflation initially, it eventually becomes smaller than the critical value ( $\approx 0.33$ ). We thus speculate that any defect comes to shrink after inflation.

In order to ascertain the above argument, we carry out numerical analysis for spherical global monopoles, using the coordinate system (1). The above arguments are verified by this numerical result: as  $\eta/m_{\text{Pl}}(\Phi)$  gets close to the critical value, the monopole stops expanding and begins to shrink.

Figure 3 shows the trajectories of the position of  $\phi = \eta/2$  for several values of  $\omega$ . The curves indicate that a monopole does not shrink toward the origin but tends to take a stable configuration.

The result that inflation eventually ends stems merely from the change of the local values of  $m_{\text{Pl}}(\Phi)$ . We may therefore extend this result to models of other topological defects.

Next, we discuss constraints for this model to be a realistic cosmological model. One of the distinguishing features of this model is that there are two scenarios of exiting from an inflationary phase and entering a reheating phase. This is illustrated by the slow-roll conditions,

$$\epsilon^{-1} \equiv \frac{\sqrt{6\pi}\eta}{m_{\text{Pl}}(\Phi)} \gg 1, \quad \text{with } \phi \ll \eta \left(1 - \frac{\epsilon}{2}\right) \equiv \phi_f. \quad (5)$$

When the condition  $\epsilon^{-1} \gg 1$  (a more precise condition is  $\eta/m_{\text{Pl}}(\Phi) > 0.33$ ) breaks down, inflation stops globally. Before this time, many local regions with the present-horizon size enter a reheating phase when

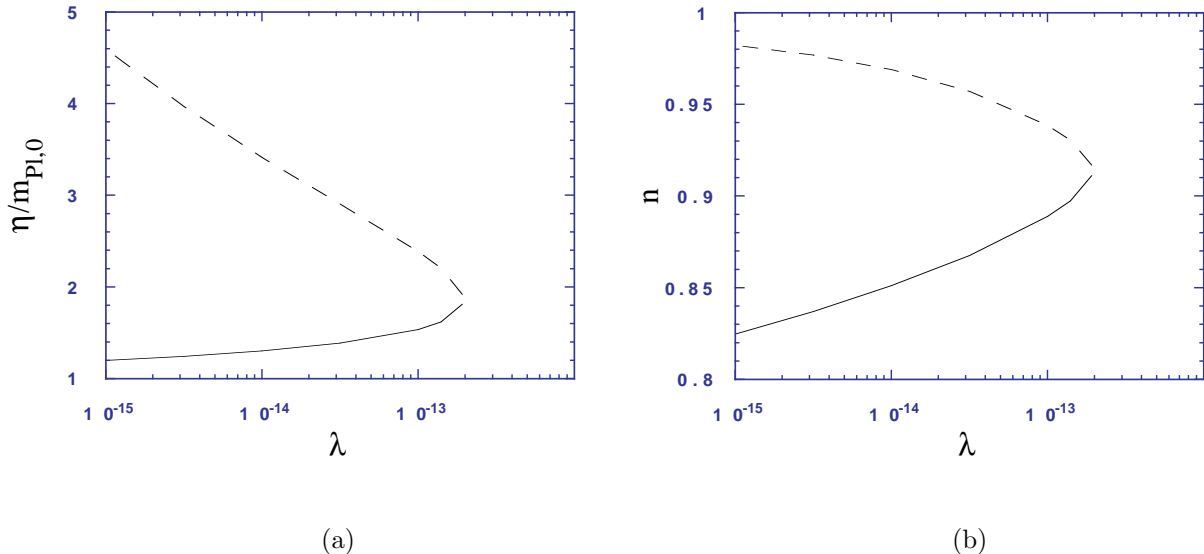


Figure 4: Constraints from COBE-normalized amplitudes of density perturbations. (a) Concordant values of  $\lambda$  and  $\eta/m_{\text{Pl},0}$ . (b) The spectral indices of density perturbations.

the second condition  $\phi \ll \phi_f$  breaks down. The second scenario is just like that of standard TDI or other slow-roll inflationary models. In the first scenario a microscopic monopole might remain in the observable universe. Unfortunately, however, this possibility turns out to be ruled out because  $\eta/m_{\text{Pl}}(\Phi_f)$  must be larger than 1 from the COBE normalization, as will be seen in Fig. 4(a) later. Thus we only consider the second (standard) reheating scenario.

Starobinsky & Yokoyama [18] derived the amplitude of a density perturbation on comoving scale  $l = 2\pi/k$  in terms of Bardeen's variable  $\Phi_A$  [19] as

$$\Phi_A(l)^2 = \frac{48V}{25m_{\text{Pl}}(\Phi)^4} \left[ \frac{8\pi V^2}{m_{\text{Pl}}(\Phi)^2 V_{,\phi}^2} + \frac{(e^{2\gamma^2 N} - 1)^2}{4\gamma^2} \right], \quad \text{with } \gamma \equiv \sqrt{\frac{2}{2\omega + 3}} \quad (6)$$

where all quantities are defined at the time  $t_k$  when the  $k$ -mode leaves the Hubble horizon, *i.e.*, when  $k = aH$ .  $N$  is defined as  $N \equiv \ln(a_f/a_k)$ , where the subscript  $f$  denotes the time at the end of inflation.

Since the large-angular-scale anisotropy of the microwave background due to the Sachs-Wolfe effect is given by  $\delta T/T = \Phi_A/3$ , we can constrain the values of  $\lambda$  and  $\eta/m_{\text{Pl}}$  by the 4yr COBE-DMR data normalization [20]:  $\Phi_A/3 \cong 10^{-5}$ , on the relevant scale. We choose  $N_{k=a_0 H_0} = 65$  typically, where a subscript 0 denotes the present epoch. Figure 4(a) shows the allowed values of  $\lambda$  and  $\eta/m_{\text{Pl}}$  for  $\gamma = 0.045$  ( $\omega = 500$ ). The concordant values are represented by two curves, which is a distinguishing feature for the double-well potential. Unfortunately, fine-tuning of  $\lambda \lesssim 10^{-13}$  is needed, just like other models [18]. The constraints for  $\omega > 500$  are practically no different from those in the Einstein gravity.

Using the relation  $d \ln k = da/a + dH/H$  and the field equations, we obtain [21]

$$n - 1 \equiv \frac{d \ln \Phi_A^2}{d \ln k} \cong -\frac{3m_{\text{Pl}}(\Phi)^2 V_{,\phi}^2}{8\pi V^2} + \frac{m_{\text{Pl}}(\Phi)^2 V_{,\phi\phi}}{4\pi V} - 6\gamma^2. \quad (7)$$

The spectral indices are plotted in Fig. 4(b); the two lines correspond to the two lines of COBE-normalized amplitudes in Fig. 4(a). As Eq. (7) suggests, the deviation from the Einstein theory is only  $6\gamma^2 \cong 0.01$  for  $\omega = 500$ . Therefore, the relatively large shift from  $n = 1$  is caused not by the BD field but by the double well potential.

Finally, we consider the detectability of relic monopoles in this model. Due to the sufficient expansion,  $N > 65$ , the core of a monopole is located so far from the observed region that even the long-range term of a global monopole,  $\rho = \eta^2/R^2$ , does not exert any effective astrophysical influence.

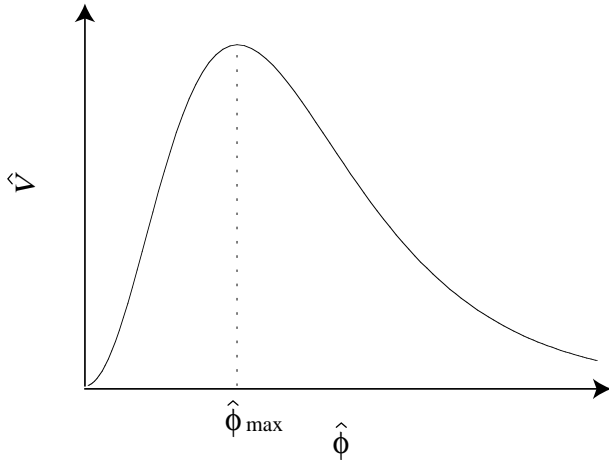


Figure 5: The potential  $\hat{V}(\hat{\phi})$  in a fictitious world for  $\xi < 0$  [22]. A plateau at  $\hat{\phi} = \hat{\phi}_{\max}$  leads TDI.

## 4 Topological Defect Inflation Induced by Non-Minimally Coupled Massive Scalar Field

The model with a non-minimally coupled massive scalar field is described by the action,

$$S = \int d^4x \sqrt{-g} \left[ \frac{\mathcal{R}}{2\kappa^2} - \frac{1}{2}\xi\phi^2\mathcal{R} - \frac{1}{2}(\nabla\phi)^2 - V(\phi) \right], \quad \text{with } V(\phi) = \frac{1}{2}m^2\phi^2 \quad \text{and} \quad \kappa^2 \equiv \frac{8\pi}{m_{\text{Pl}}^2}. \quad (8)$$

Futamase & Maeda [22] investigated how the nonminimal coupling term  $(1/2)\xi\mathcal{R}\phi^2$  affects realization of chaotic inflation [23], and derived constraints on the coupling constant  $\xi$  from the condition for sufficient inflation. For the massive scalar model (8), they obtained  $|\xi| \lesssim 10^{-3}$ . Here we show that another type of inflation may be possible if  $\xi < 0$ , which relaxes the constraint on  $\xi$ .

Following Futamase & Maeda, we apply the conformal transformation and redefine a scalar field so that the model is described by the Einstein gravity with a canonical scalar field:

$$\hat{S} = \int d^4\hat{x} \sqrt{-\hat{g}} \left[ \frac{\hat{\mathcal{R}}}{2\kappa^2} - \frac{1}{2}(\hat{\nabla}\hat{\phi})^2 - \hat{V}(\hat{\phi}) \right], \quad \text{with } \hat{V}(\hat{\phi}) = \frac{V(\phi)}{(1+\psi)^2} \quad \text{and} \quad \psi \equiv -\xi\kappa^2\phi^2. \quad (9)$$

Thanks to this standard form of the theory, we can discuss the qualitative behavior of  $\hat{\phi}$  (or  $\phi$ ) in terms of the potential shape. We depict  $\hat{V}(\hat{\phi})$  for  $\xi < 0$  in Fig. 5. A distinguishing feature of this potential is that it has a maximum at  $\hat{\phi} = \hat{\phi}_{\max}$  corresponding to  $\psi = 1$  or  $\phi = 1/\kappa\sqrt{-\xi} \equiv \phi_{\max}$ . Hence, if the initial value of the scalar field,  $\hat{\phi}_i$ , is larger than  $\hat{\phi}_{\max}$  and if the energy density of the scalar field  $E_{\hat{\phi}} = \hat{\phi}_{,t}^2/2 + \hat{V}(\hat{\phi})$  is below  $\hat{V}(\hat{\phi}_{\max})$ ,  $\hat{\phi}$  cannot reach the origin  $\hat{\phi} = \phi = 0$ , but it will run away to infinity as long as the universe is expanding in the conformal frame with  $\hat{H} > 0$ . This runaway solution is irrelevant to our Universe, and Futamase & Maeda [22] obtained a constraint  $|\xi| < 10^{-3}$  so that  $\hat{\phi}_{\max} > 5m_{\text{Pl}}$  and the initial value of  $\hat{\phi}$  required for sufficient chaotic inflation  $\hat{\phi}_i \sim 5m_{\text{Pl}}$  lies on the left of the potential peak.

We can argue, however, that sufficient inflation may be possible even if  $\hat{\phi}_{\max} < 5m_{\text{Pl}}$  because the plateau around  $\hat{\phi} = \hat{\phi}_{\max}$  may cause another channel of inflation. Seen in the conformal frame, some domains of the universe relax to  $\hat{\phi} = 0$  and others run away to  $\hat{\phi} \rightarrow \infty$  as the universe expands. In between these two classes of regions exist domain walls where large potential energy density  $\hat{V}(\hat{\phi}_{\max})$  is stored. If the curvature of the potential is sufficiently small there, such domain walls will inflate. This is nothing but TDI.

Let us discuss whether inflation can take place at  $\hat{\phi} = \hat{\phi}_{\max}$ , following the arguments of Linde & Vilenkin [2]. The standard conditions for slow-roll inflation lead to

$$\frac{|\xi|}{1+3|\xi|} \ll \frac{3}{4}. \quad (10)$$

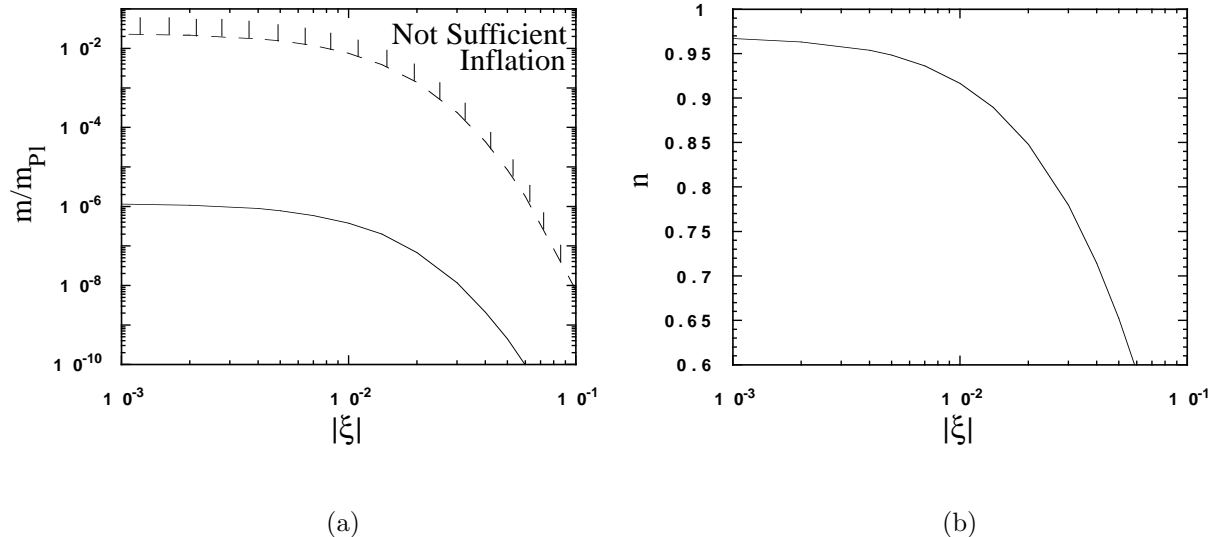


Figure 6: Constraints from COBE-normalized amplitudes of density perturbations. (a) Constraints on  $\xi$  and  $m/m_{\text{Pl}}$ . The dashed curve is a constraint from sufficient inflation. The solid curve represents the concordant values with the amplitude of the COBE-DMR data. (b) The spectral indices of density perturbations.

A similar relation is derived from the condition that the thickness of the wall characterized by the curvature scale of the potential at the maximum,  $\hat{R}_w$ , is greater than the horizon,  $\hat{H}^{-1}$ :

$$\hat{R}_w \hat{H} = \sqrt{\frac{\kappa^2 \hat{V}(\hat{\phi}_{\text{max}})}{3 \hat{V}_{,\hat{\phi}\hat{\phi}}(\hat{\phi}_{\text{max}})}} = \sqrt{\frac{1+3|\xi|}{12|\xi|}} \gtrsim 1. \quad (11)$$

Inequalities (10) and (11) suggest that inflation actually takes place at the top of the potential if  $|\xi| \ll 1$ . Once inflation sets in, it continues forever inside a domain wall.

In order to obtain more precise conditions for sufficient inflation, we solve the (homogeneous and isotropic) field equations numerically. We assume initial values as  $\hat{\phi}_i = \delta\hat{\phi}_Q \equiv \hat{H}/2\pi$  and  $(\hat{\phi}_{,\hat{t}})_i = 0$ , and observe the e-fold number of inflation after the classical dynamics dominates over quantum fluctuations, *i.e.*,  $|\hat{\phi}_{,\hat{t}}|/\hat{H} > \delta\hat{\phi}_Q$ . Sufficient expansion typically requires  $a_f/a_c > e^{65}$ , where  $c$  denotes the time when  $|\hat{\phi}_{,\hat{t}}|/\hat{H} = \delta\hat{\phi}_Q$ . The allowed region is plotted in Fig. 6(a). This shows that inflation continues sufficiently even if  $|\xi| \cong 0.1$ , contrary to the previous result [22].

Next, we investigate density perturbations generated during inflation, and constrain the model from the 4yr COBE-DMR data [20]. Because Makino & Sasaki [24] showed that the density perturbation in the original frame exactly coincides with that in the conformal frame, we can easily calculate the amplitude and the spectral index with the well-known formulas. The amplitude of perturbation is given as

$$\Phi_A \left( l = \frac{2\pi}{k} \right) = \frac{\sqrt{3}\kappa^3 \hat{V}^{\frac{3}{2}}}{10\pi \hat{V}_{,\hat{\phi}}} = \frac{\sqrt{3}\kappa^3 m \hat{\phi}^2 \sqrt{1+(1-6\xi)\psi}}{20\sqrt{2}\pi(1-\psi^2)}. \quad (12)$$

The large-scale anisotropy of the cosmic microwave background measured by COBE-DMR leads to [20]  $\delta T/T = \Phi_A/3 \cong 10^{-5}$ . The concordant values of  $\xi$  and  $m$  are also plotted in Fig. 6(a).

The spectral index  $n$  is given as [21]

$$n - 1 \equiv \frac{d \ln \Phi_A^2}{d \ln k} = \frac{4}{\kappa^2 \hat{\phi}^2} \left[ -\frac{3(1-\psi)^2}{1+(1-6\xi)\psi} + \frac{1-6\psi-(5-35\xi)\psi^2+2(1-6\xi)\psi^3}{\{1+(1-6\xi)\psi\}^2} \right]. \quad (13)$$

The values of  $n$  which satisfy the COBE-DMR normalization are plotted in Fig. 6(b). With the observational data,  $n = 1.2 \pm 0.3$  [20], we have a constraint  $|\xi| \lesssim 10^{-2}$ , which is still less stringent than the previous result [22].

## Acknowledgments

I would like to thank Tomohiro Harada, Kei-ichi Maeda, Ken-ichi Nakao, and Jun'ichi Yokoyama, with whom the present work was done. Thanks are also due to Paul Haines for reading the manuscript. Numerical Computation of this work was carried out at the Yukawa Institute Computer Facility. I was supported by JSPS Research Fellowships for Young Scientist, No. 9702603.

## References

- [1] E.I. Guendelman & A. Rabinowitz, *Phys. Rev. D.* **44**, 3152 (1991).
- [2] A. Linde, *Phys. Lett. B* **327**, 208 (1994); A. Vilenkin, *Phys. Rev. Lett.* **72**, 3137 (1994).
- [3] N. Sakai, H. Shinkai, T. Tachizawa & K. Maeda, *Phys. Rev. D* **53**, 655 (1996).
- [4] N. Sakai, *Phys. Rev. D* **54** 1548 (1996).
- [5] J. Ellis, N. Kaloper, K.A. Olive & J. Yokoyama, *Phys. Rev. D* **59**, 103503 (1999); Izawa K.-I., M. Kawasaki & T. Yanagida, *Prog. Theor. Phys.* **101**, 1129 (1999).
- [6] N. Sakai, K. Nakao & T. Harada, preprint gr-qc/9909027.
- [7] N. Sakai, J. Yokoyama & K. Maeda, *Phys. Rev. D* **59**, 103504 (1999).
- [8] N. Sakai & J. Yokoyama, *Phys. Lett. B* **456**, 113 (1999).
- [9] For a review of spacetime solutions with non-Abelian fields, see, e.g., M.S. Volkov & D.V. Gal'tsov, preprint hep-th/9810070.
- [10] M.E. Ortiz, *Phys. Rev. D* **45**, R2586 (1992); K. Lee, V.P. Nair & E.J. Weinberg, *ibid.* **45**, 2751 (1992); P. Breitenlohner, P. Forgács & D. Maison, *Nucl. Phys.* **B383**, 357 (1992); *ibid.* **B442**, 126 (1995).
- [11] T. Tachizawa, K. Maeda & T. Torii, *Phys. Rev. D* **51**, 4054 (1995).
- [12] A. Borde, M. Trodden & T. Vachaspati, *Phys. Rev. D* **59**, 43513 (1998); T. Vachaspati & M. Trodden, preprint gr-qc/9811037.
- [13] T. Nakamura, K. Oohara & Y. Kojima, *Prog. Theor. Phys. Suppl.* **90**, 1 (1987).
- [14] K. Sato, M. Sasaki, H. Kodama & K. Maeda, *Prog. Theor. Phys.* **65**, 1443 (1981); K. Sato, H. Kodama, M. Sasaki & K. Maeda, *ibid.* **108B**, 103 (1982).
- [15] K. Sato, *Mon. Not. Roy. Astron. Soc.* **195**, 467 (1981); *Phys. Lett.* **99B**, 66 (1981); A.H. Guth, *Phys. Rev. D* **23**, 347 (1981).
- [16] I. Cho & A. Vilenkin, *Phys. Rev. D* **56**, 7621 (1997).
- [17] D. La & P.J. Steinhardt, *Phys. Rev. Lett.* **62**, 376 (1989).
- [18] A. Starobinsky & J. Yokoyama, *Proc. 4th Workshop on General Relativity and Gravitation* eds. K. Nakao *et al.* (Yukawa Institute for Theoretical Physics), 381 (1994).
- [19] J.M. Bardeen, *Phys. Rev. D* **22**, 1882 (1980).
- [20] C.L. Bennet *et al.*, *Astrophys. J.* **464**, L1 (1996).
- [21] A.R. Liddle & D.H. Lyth, *Phys. Lett. B* **291**, 391 (1992).
- [22] T. Futamase & K. Maeda, *Phys. Rev. D* **39**, 399 (1989).
- [23] A. Linde, *Phys. Lett. B* **129**, 177 (1983).
- [24] N. Makino & M. Sasaki, *Prog. Theor. Phys.* **86**, 103 (1991).